Title

Synthetic Antimicrobial Peptide Tuning Permits Membrane Disruption and Interpeptide Synergy

Journal

ACS Pharmacology & Translational Science, 3(3)

ISSN

2575-9108

Authors

Fields, Francisco R
Manzo, Giorgia
Hind, Charlotte K
et al.

Publication Date

2020-06-12

DOI

10.1021/acsptsci.0c00001

Peer reviewed

ACS Pharmacology & Translational Science

pubs.acs.org/ptsci Letter

Synthetic Antimicrobial Peptide Tuning Permits Membrane Disruption and Interpeptide Synergy

Francisco R. Fields, Giorgia Manzo, Charlotte K. Hind, Jeshina Janardhanan, Ilona P. Foik, Phoebe Do Carmo Silva, Rashna D. Balsara, Melanie Clifford, Henry M. Vu, Jessica N. Ross, Veronica R. Kalwajtys, Alejandro J. Gonzalez, Tam T. Bui, Victoria A. Ploplis, Francis J. Castellino, Albert Siryaporn, Mayland Chang, J. Mark Sutton, A. James Mason, and Shaun Lee*

Cite This: *ACS Pharmacol. Transl. Sci.* 2020, 3, 418–424 Read Online

ACCESS | Metrics & More | Article Recommendations | Supporting Information

ABSTRACT: The ribosomally produced antimicrobial peptides of bacteria (bacteriocins) represent an unexplored source of membrane-active antibiotics. We designed a library of linear peptides from a circular bacteriocin and show that pore-formation dynamics in bacterial membranes are tunable via selective amino acid substitution. We observed antibacterial interpeptide synergy indicating that fundamentally altering interactions with the membrane enables synergy. Our findings suggest an approach for engineering pore-formation through rational peptide design and increasing the utility of novel antimicrobial peptides by exploiting synergy.

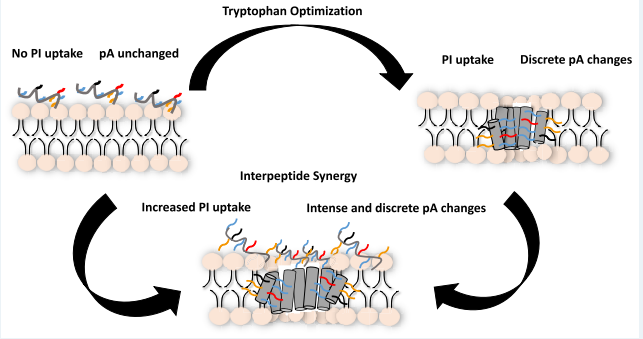

KEYWORDS: *antimicrobial peptides, bacteriocins, synergy*

Bacteriocins, the ribosomally produced peptides of bacteria, represent a potentially vast source of novel templates for the design of antimicrobials, with their discovery aided by recent advances in human genomic and microbiome research.[1−3] The class I bacteriocin AS-48 may hold significant potential as a simple peptide scaffolds for the development and optimization of antimicrobial compounds.[4−7] Enterocin AS-48, first isolated from *Enterococcus faecalis* AS-48, is a circular bacteriocin consisting of five helical domains with an overall positive charge.[6,8] These basic residues cluster within helices four and five are designated as the membrane targeting region.[6,9,10] Previous studies have shown that antimicrobial activity is specifically dependent upon the hydrophobic residues in this region, the amino acid structure of which resembles the biochemical design of many cationic, helical, and hydrophobic eukaryotic and synthetic antimicrobial peptides (AMPs).[6,9,10] These studies suggest that natural bacteriocins, often too large for chemical synthesis, can be minimized to a short core domain for rapid synthesis and development of novel antimicrobial compounds.

Previously, we demonstrated that the membrane-interacting region of an AS-48 homologue, safencin AS-48, can serve as a simple linear peptide template for library optimization.[11] This artificial peptide, termed syn-safencin, was modified by selective substitution with lysine and tryptophan to create 96 synthetic peptides. Of the 96 peptides screened for antimicrobial activity, we discovered two glycine to tryptophan substitutions at key sites correlating with the highest antimicrobial activity. To gain a more fundamental understanding of how selective amino acid substitutions of minimal synthetic bacteriocin peptides influence antimicrobial activity, we performed detailed biophysical studies on several synthetic AMPs and evaluated the effect of selective amino acid substitutions on the mechanism of bacterial membrane disruption within our optimized peptides series.

Red residues indicate an amino acid change relative to the parent peptide

From our initial syn-safencin library we designated a group of five peptides for further characterization. These include the syn-safencin parent peptide (designated SynSaf-P1) and a set of similar peptides with stepwise amino acid substitutions derived from the most active SynSaf-P1 variant, the SynSaf-P96 series. (Table 1). All of the peptide candidates exhibited strong antimicrobial activity when tested against a panel of agriculturally and clinically relevant Gram-negative bacteria, with no detectable cytotoxicity or hemolytic activity (Table S-

Special Issue: Antibiotics

Received: January 3, 2020
Published: February 21, 2020

Table 1. Syn-safencin Peptides Selected for Study

Parent Peptide (Syn-safencin)	
SynSaf-P1	AGKETIRQYLKNEIKKKGRKAVIAW
SynSaf-P96 Series	
SynSaf-P8	AGKEKIRKKLKNEIKKKGRKAVIAW
SynSaf-P24	AWKEKIRKKLKNEIKKKGRKAVIAW
SynSaf-P56	AGKEKIRKKLKNEIKKKWRKAVIAW
SynSaf-P96	AWKEKIRKKLKNEIKKKWRKAVIAW

1, Figures S-1 & S-2). Increasing the overall charge in the SynSaf-P96 series with lysine (SynSaf-P8) did not significantly alter antimicrobial activity as compared to the SynSaf-P1 (Table S-1). However, tryptophan substitution at particular residues significantly affected the overall antibacterial activity with respect to the parent sequence. For SynSaf-P24, with the G2W substitution, and SynSaf-P56, with the G18W substitution, antibacterial activity, measured by minimum inhibitory concentration (MIC), was significantly reduced against multiple bacterial species (Table 1 and Table S-1). However, peptides with the G18W mutation exhibited greater antimicrobial activity than their G2W counterparts (Table S-1). Inclusion of both G2W and G18W substitutions in SynSaf-P96 significantly enhanced the antimicrobial activity against both *Klebsiella pneumoniae* strains tested and *Pseudomonas aeruginosa* PAO1 (Table 1 and Table S-1). No appreciable activity was observed against a panel of Gram-positive bacteria (Table S-2). Next, we evaluated the MICs of the most effective peptides, against clinically relevant isolates of *E. coli* and *A. baumannii* (Table S-3). Again, we observed lower MICs for SynSaf-P56 compared to SynSaf-P96 which had both of the tryptophan substitutions.

We hypothesized that the tryptophan-dependent increase in the antimicrobial activity of the peptide series may correlate with their increased ability to permeate Gram-negative bacterial membranes. Fluorescence assisted cell sorting (FACS) using propidium iodide (PI) treated *Escherichia coli* BL-21 showed an increase in PI uptake with peptides that

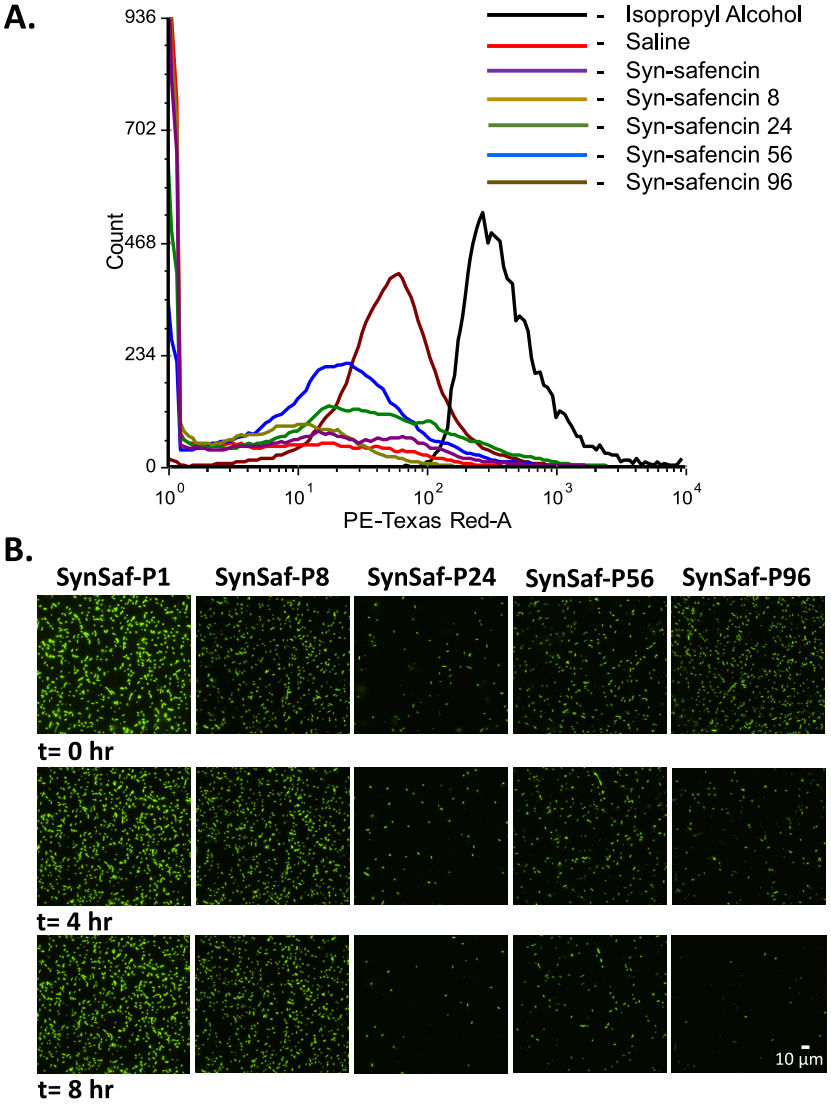

Figure 1. Systematic amino acid substitutions in Syn-safencin increase its membrane disrupting capacity. (A) PI FACs sorting histograms of *E. coli* BL-21 treated with 20 μM peptide. Isopropyl alcohol, saline, SynSaf-P1, P8, P24, P56, and P96 are in black, red, purple, gold, green, blue, and brown, respectively. Histograms are representative of three replicates (n = 3). (B) GFP expressing *E. coli* treated with 10 μM peptide (columns) for 0 (top), 4 (middle), and 8 (bottom) hours. Images are representative of two replicates (n = 2).

https://dx.doi.org/10.1021/acsptsci.0c00001
ACS Pharmacol. Transl. Sci. 2020, 3, 418−424

contained tryptophan substitutions, confirming that tryptophan substitution enhanced peptide mediated membrane permeabilization (Figure 1A). We further supported these data with live-imaging experiments, wherein green fluorescent protein (GFP)-expressing *E. coli* BL-21 was incubated with the peptide candidates and imaged live for 8 h. Our results indicated that the parent peptide, SynSaf-P1, was unable to induce significant membrane leakage over 8 h, as evidenced by retention of GFP (Figure 1B). Similar results were observed for the lysine optimized peptides SynSaf-P4 and SynSaf-P8. However, a rapid loss of GFP was observed when incubated with all tryptophan substituted peptide candidates (Figure 1B).

To determine the effect of tryptophan substitution on key biophysical characteristics of the SynSaf peptides, a detailed investigation of secondary structure and pore formation dynamics was conducted on each of the peptides in Gram-negative model membranes.[12−19] All CD studies were performed using small unilamellar vesicles (SUVs) consisting of phosphatidylethanolamine and phosphatidylglycerol (POPE:POPG) while 2-D NMR structures were obtained in sodium dodecyl sulfate (SDS) micelles. All patch clamp experiments were performed on lipid bilayers consisting of diphytanoylphosphatidylethanolamine and diphytanoylphosphatidylglycerol (DPhPE:DPhPG). The parent peptide, SynSaf-P1, adopted a helical conformation in POPE:POPG vesicles with bands at 208 and 222 nm (Supplemental Figure 3A). The NMR structure reveals that this helicity is concentrated toward the C-terminus of the peptide (Supplemental Figure 3A). However, no appreciable membrane disruption was observed in the patch clamp experiments (Supplemental Figure 3B).

Upon lysine optimization, SynSaf-P8 shifted toward an unstructured conformation in POPE:POPG with a single band near 200 nm (Figure 2A). A similar trend is observed in the NMR structure with SynSaf-P8 adopting a more unstructured conformation compared to SynSaf-P1. This likely occurs through electrostatic repulsion as the lysine substitutions are located in close proximity to other basic residues.[20] While the charge optimization step did not confer any pore forming capability to SynSaf-P8 it did increase the latency time, the time to membrane activity upon peptide administration, of SynSaf-P8 compared to SynSaf-P1 (Figure 2B and Figure S-7). This indicates that, upon lysine addition, the peptides decrease their affinity for the bacterial membrane despite its negative surface charge. These observations explain the lack of biological activity observed with SynSaf-P8 in the live imaging, FACs, and MIC experiments (Figure 1 and Table S-1).

Peptides with substitutions of W at G2 or G18 (SynSaf-P24, SynSaf-P56) adopted a helical structure (Figures S-4A and S-5A). Discrete membrane events were observed for the peptides containing either W substitution (Figures S-4B and S-5B). For SynSaf-P24 (G2W replacement) channel-like activity, similar to other pore-forming peptides, was observed, with two populations of event intensities around 0.5 and 1.5 pA (Figure S-4B).[19,21] SynSaf-P56 (G18W substitution) exhibited strong membrane disrupting activity with a large population of events around 3pA. However, these events did not appear to be as strongly defined as SynSaf-P24 (Figure S-5B)

SynSaf-P96 exhibited a helical signature that was markedly different from the parent peptide, indicating a shift in the helical content with both W substitutions (Figure 3A and Figure S-3A). SynSaf-P96 was shown to be highly structured at its N-terminus with a weaker helical conformation toward the

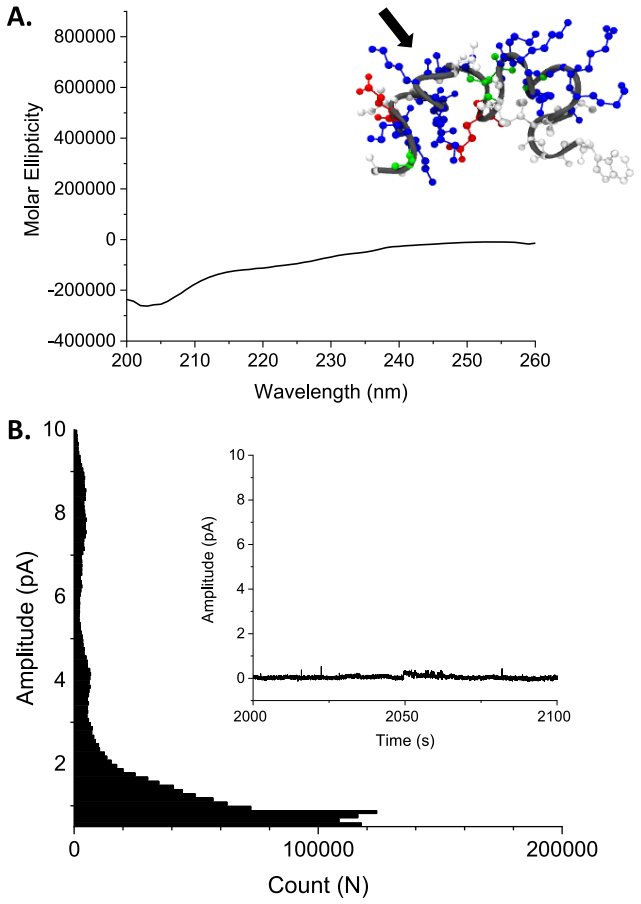

Figure 2. Syn-safencin 8 (SynSaf-P8) is an unstructured, non-membrane disrupting peptide. (A) Secondary structure interrogation of SynSaf-P8 indicates that it is an unstructured peptide. CD data were collected in the presence of POPE:POPG SUVs. 2-D NMR structure of SynSaf-P8 determined in SDS micelles (inset) PDB accession number 608P. Arrows indicate the region of increased positive charge due to the amino acid substitutions in Table 1. Basic, acidic, polar, and hydrophobic residues are in blue, red, green, and white, respectively. (B) SynSaf-P8 does not disrupt Gram negative model membranes, at 40 μM, as indicated by patch clamp. The all-data point histogram and example trace (inset) of SynSaf-P8 are representative of six experiments (n = 6) on DPhPE:DPhPG bilayers.

C-termini (Figure 3A). The extension of helical content along most of its length likely contributes to its pronounced ability to disrupt the bacterial membrane as observed in FACS (Figure 1). Interestingly, we did not observe similar secondary structural differences between the SynSaf peptides in a Gram-positive mimicking environment (POPG SUVs) (Figure S-6). This in concert with previous MIC data may indicate that our previously described optimization method may have imparted some specificity toward the Gram-negative membrane (Tables S-1, S-2, and S-3).

SynSaf-P96, with both G2W and G18W replacements, also strongly disrupted models of Gram-negative membranes in patch clamp experiments giving rise to five discrete populations of events from 0.5 pA to 17 pA; however, these events included discrete channel formation, akin to SynSaf-P24, and indiscriminate intense events, akin to SynSaf-P56 (Figure 3B insert, Figure S-4B inset, and Figure S-5B inset).[17−19,21] Using the five levels of events identified, estimated pore sizes were calculated for the SynSaf-P96 series.[21] Similar pore sizes were observed for SynSaf-P1 and SynSaf-P8, but for peptides with the G18W

https://dx.doi.org/10.1021/acsptsci.0c00001
ACS Pharmacol. Transl. Sci. 2020, 3, 418−424

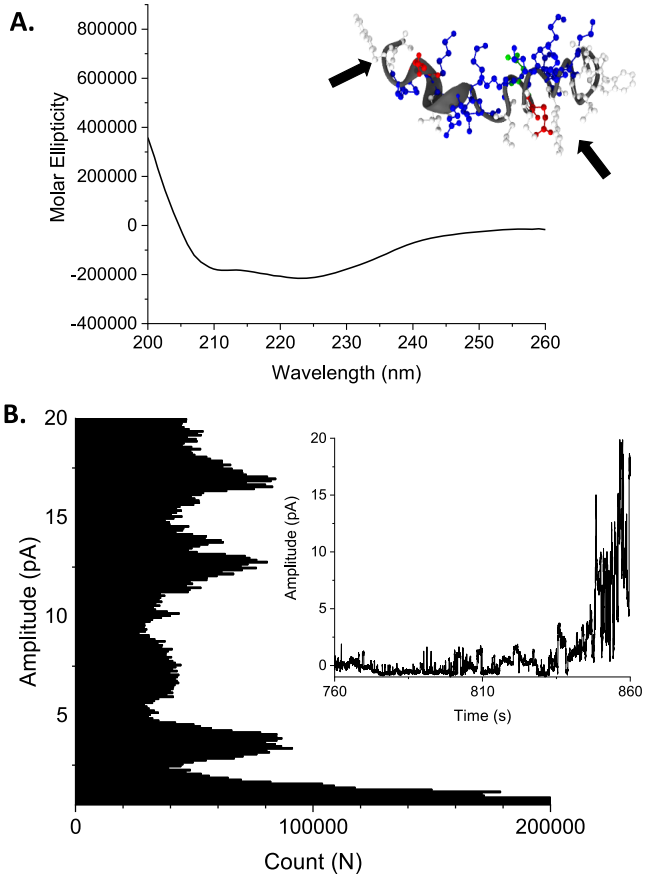

Figure 3. Syn-safencin 96 (SynSaf-P96) is a helical, pore forming antimicrobial peptide. (A) Secondary structure interrogation of SynSaf-P96 indicates that it is a helical peptide. CD data was collected in the presence of POPE:POPG SUVs. 2-D NMR structure of SynSaf-P96 determined in SDS micelles (inset). PDB accession number 608S. Arrows indicate the G2W and G18W substitutions noted in Table 1. Basic, acidic, polar, and hydrophobic residues are in blue, red, green, and white, respectively. (B) SynSaf-P96 strongly disrupts Gram negative model membranes, at 40 μM, as indicated by patch clamp. The data point histogram and example trace (inset) of SynSaf-P96 are representative of six experiments (n = 6) on DPhPE:DPhPG bilayers.

substitution, SynSaf-P56 and SynSaf-P96, level one pores were larger than those for the other peptides with radii equal to 0.082 and 0.067 nm respectively (Table S-4). Despite the location dependent effects of pore formation, this had no effect on the latency time with tryptophan addition significantly reducing the latency time compared to their nontryptophan optimized counterparts (SynSaf-P1 and SynSaf-P8) (Figure S-7).

We noted that although some peptide candidates were unable to induce membrane disruption, they still exhibited significant antimicrobial activity, suggesting that these peptides may adopt an alternative antimicrobial mechanism of action. For example, SynSaf-P8 did not induce membrane disruption in our experiments. Nonetheless, this agent showed strong antibacterial activity against the plant pathogens, *Pseudomonas syringae* and *Xanthomonas axonopodis,* with MICs of 1 and 4 μg/mL, respectively, and weak antimicrobial activity against *Acinetobacter baumannii* AYE, MIC ~ 64 μg/mL (Table S-1). To determine whether alternative mechanisms of antimicrobial activity exhibited by our SynSaf peptides could display synergistic antibacterial effects, we investigated peptide−peptide synergy using a comprehensive MIC-based assay of peptide combinations. We reasoned that small amino acid changes that fundamentally altered the pore-forming mechanism of action within our library would display synergistic effects, as they have adopted a distinct mechanism of action from SynSaf-P1. We observed multiple synergistic interactions within the SynSaf-P96 series against *E. coli* NCTC 12923 and *A. baumannii* AYE (Table S-5). These synergistic interactions were consistent for SynSaf-P96 in combination with SynSaf-P1, -P8, and -P24 (Table S-5). The interaction between SynSaf-P8 and SynSaf-P96 was determined to be strongly synergistic using a full checkerboard assay (FICI = 0.31 ± 0.08). This activity was similar to the FICI value for PGLa and magainin, two naturally synergistic frog AMPs, which is 0.3 against *E. coli*.[22] The synergistic interaction was further interrogated via patch clamp and FACS analysis. Synergy is detected in FICI assays when the effective concentration of both compounds can be reduced at least 4-fold in combination. SynSaf-P8 shows no membrane activity in patch clamp or FACs analysis when used at a much lower concentration (Figure S-8A and Figure 4A). At a reduced concentration, SynSaf-P96 retains pore forming activity as indicated by patch clamp with two populations at 0.5 and 2 pA (Figure S-8B). This is reflected

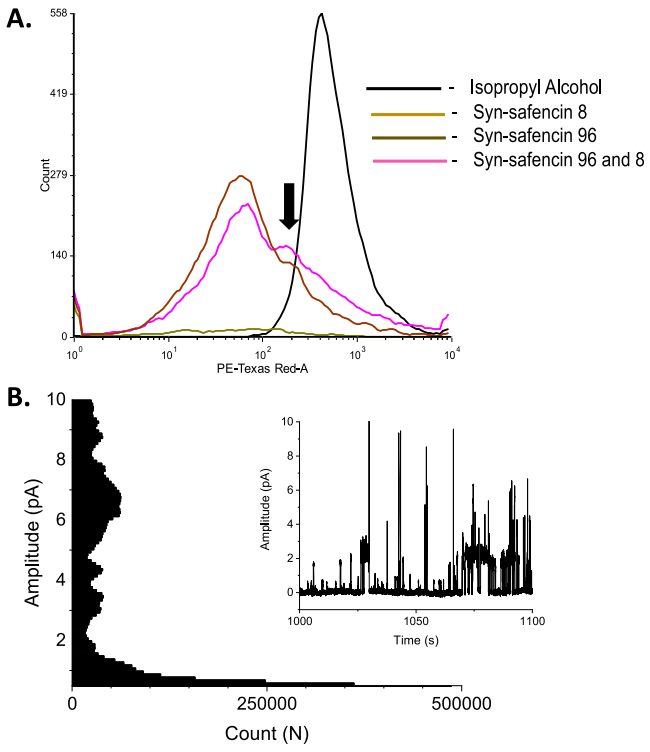

Figure 4. Synergy between the nonpore forming SynSaf-P8 and the pore-forming SynSaf-P9, results as a consequence of tryptophan optimization. (A) Synergy condition results in a shift toward a higher fluorescent intensity of treated *E. coli* via PI FACS. Cells were treated with 5 μM peptide alone or 5 μM of each for the synergy condition. Arrow indicates the population of higher fluorescent intensity. Isopropyl alcohol, SynSaf-P8, P96, or P8, and P96 are in black, gold, brown, and pink, respectively. Histogram is representative of three replicates (n = 3). (B) Synergy results in discrete pore formation. SynSaf-P8 and SynSaf-P96, both at 10 μM, were used to treat DPhPE:DPhPG bilayers. The data point histogram and trace (inset) are representative of six replicates (n = 6).

https://dx.doi.org/10.1021/acsptsci.0c00001
ACS Pharmacol. Transl. Sci. 2020, 3, 418−424

in our FACS analysis with a single population of PI positive *E. coli* (Figure 4A). Upon treatment with both peptides, a second population of higher fluorescent intensity emerges in FACS (Figure 4A). Consistently, new populations of high amplitude pores appear in patch clamp (Figure 4B). Level-2 pores were formed in the synergy condition that were larger than those formed by SynSaf-P96 alone, (0.125 and 0.096 nm respectively) (Table S-6). These data indicate that SynSaf-P8, a nonpore forming peptide, enhances the pore forming capability of SynSaf-P96. To further investigate the synergistic mechanism of Gram-negative membrane disruption, we interrogated the membranes of *P. aeruginosa* PAO1 treated with SynSaf-P8 and -P96 using transmission electron microscopy (Figure 5A). Similar to other TEM images of *P. aeruginosa*, we observed intact membranes in the untreated control (Figure 5A).[23,24] SynSaf-P8 and -P96 both caused membrane disruptions compared to the untreated control; however, the observed disruptions were different. SynSaf-P8 caused minor disruptions in the membrane with small leakage events (Figure 5A). For SynSaf-P96, we observed membrane "bundling" events across the surface of the bacteria (Figure 5A). When the concentrations of the peptides are reduced by a fourth for the synergy condition, we observed a unique membrane phenotype in which there were large membrane disruptions and dramatic membrane bundles (Figure 5A). These data indicate, in our synergistic conditions, that both SynSaf-P8 and SynSaf-P96 enhance each other's unique membrane-based mechanisms of action. Recent publications have proposed that AMPs act synergistically by forming heterodimers that accelerate and enhance pore formation.[25] While the exact mechanism by which synergy occurs in our synthetic peptide series is unknown, SynSaf-P8 could alter the local charge of the bacterial membrane without fully penetrating the membrane providing a more energetically favorable surface to allow SynSaf-P96 to form pores more efficiently and deform the membrane at lower concentrations.

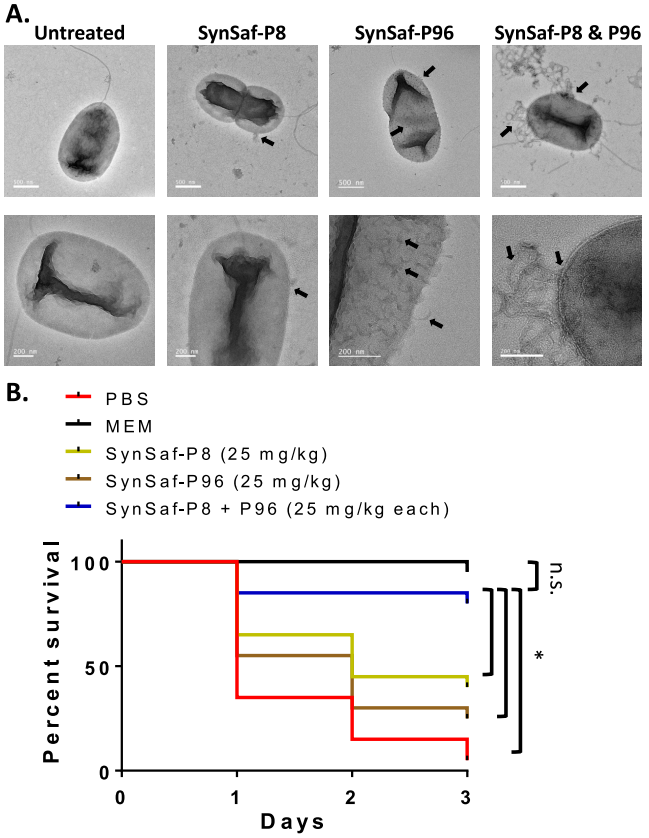

Figure 5. SynSaf-P8 and SynSaf-P96 synergize *in vivo*. (A) TEM images of peptide treated *P. aeruginosa* PAO1. Bacteria were treated with 20 μM peptide or 5 μM of both peptides for the synergy condition. Arrow indicates sites of membrane disruption. (B) *In vivo* synergy in *A. baumannii* AYE infected *G. mellonella* larvae. SynSaf-P8 and SynSaf-P96 were both administered at 25 mg/kg, and the peptide combination included 25 mg/kg of each peptide (n = 20). Meropenem (MEM), PBS, SynSaf-P8, P96, or P8 and P96 are in black, red, gold, brown, and blue, respectively. An asterisk (*) indicates a significant difference according to a Mantel-Cox Test using a Bonferronni corrected alpha value (p < 0.0125). The abbreviation "n.s." indicates no significant difference.

To determine if the syn-safencin peptides could synergize *in vivo*, we utilized the *G. mellonella* model of infection using *A. baumannii* AYE. Initial toxicity studies indicate that the peptides are nontoxic when injected into the hemolymph of the uninfected larvae with only one death in the SynSaf-P1 treated group (Table S-7). Single formulations of the SynSaf peptides at a 100 mg/kg dose were unable to increase survivorship in the *A. baumannii* infected larvae (20−50% survival) to a level similar to the Meropenem control group (90% survival) over the course of the three-day infection (Figure S-9). For the synergy study, peptide concentration was reduced by a fourth to a 25 mg/kg dose with the synergy condition consisting of 25 mg/kg each of SynSaf-P8 and -P96. For the single peptide 25 mg/kg doses, we observed only 40% and 20% survival for the SynSaf-P8 and SynSaf-P96; however, a significant increase to 80% survival was observed for the synergy condition when compared to the PBS or single peptide formulations (Figure 5B). This could indicate that synergistic combinations of peptides not only increase the efficacy of the compounds but may also provide additional *in vivo* stability to antimicrobial peptides.

Our studies show how systematic amino acid substitutions in reductive linear variants of natural bacteriocins can be utilized as a heuristic approach for the design and development of novel antimicrobials. Our data suggest that full-length bacteriocins can be reductively optimized for rapid synthesis of small peptide variants that can be screened for improved activity. Furthermore, our findings show that single amino acid substitutions can alter the fundamental mechanism of action by which these peptides exert antibacterial activity. Library optimization and synergistic evaluation of peptides in SAR studies, such as those described herein, will improve the discovery of novel antimicrobial compounds that can be further developed for drug formulations. We highlight that evaluating bacteriocin-derived peptide libraries for synergy may uncover new modalities for therapeutic treatment of bacterial disease, especially given that many natural bacteriocins require two peptides in order to become fully active against their target species.[26,27] Including these approaches in future SAR evaluation of AMPs can allow for the deliberate engineering of synergistic peptide combinations. As peptides continue to be explored as novel antimicrobials, systematic approaches to reductively design bacteriocins variants and determine their mechanism of action hold enormous potential for developing rational-based approaches to AMP discovery.

https://dx.doi.org/10.1021/acsptsci.0c00001
ACS Pharmacol. Transl. Sci. 2020, 3, 418−424

■ ASSOCIATED CONTENT

Supporting Information

The Supporting Information is available free of charge at https://pubs.acs.org/doi/10.1021/acsptsci.0c00001.

Materials and Methods and additional Figures and Tables (PDF)

■ AUTHOR INFORMATION

Corresponding Author

Shaun Lee − *Department of Biology, Eck Institute of Global Health, and Chemistry Biology Biochemistry Interface, University of Notre Dame, Notre Dame, Indiana 46556, United States;* orcid.org/0000-0001-9305-2050; Email: lee.310@nd.edu

Authors

Francisco R. Fields − *Department of Biology, Eck Institute of Global Health, and Chemistry Biology Biochemistry Interface, University of Notre Dame, Notre Dame, Indiana 46556, United States;* orcid.org/0000-0002-9029-5150

Giorgia Manzo − *Institue of Pharmaceutical Science, School of Cancer & Pharmaceutical Science, King's College London, London SE1 9NH, United Kingdom*

Charlotte K. Hind − *Technology Development Group, National Infection Service, Public Health England, Salisbury SP4 0JG, U.K.*

Jeshina Janardhanan − *Department of Chemistry and Biochemistry, University of Notre Dame, Notre Dame, Indiana 46556, United States*

Ilona P. Foik − *Department of Physics and Astronomy, University of California Irvine, Irvine, California 92697, United States*

Phoebe Do Carmo Silva − *Technology Development Group, National Infection Service, Public Health England, Salisbury SP4 0JG, U.K.*

Rashna D. Balsara − *Department of Chemistry and Biochemistry and W.M. Keck Center for Transgene Research, University of Notre Dame, Notre Dame, Indiana 46556, United States*

Melanie Clifford − *Technology Development Group, National Infection Service, Public Health England, Salisbury SP4 0JG, U.K.*

Henry M. Vu − *Department of Biology and W.M. Keck Center for Transgene Research, University of Notre Dame, Notre Dame, Indiana 46556, United States*

Jessica N. Ross − *Department of Biology and Eck Institute of Global Health, University of Notre Dame, Notre Dame, Indiana 46556, United States*

Veronica R. Kalwajtys − *Department of Biology, University of Notre Dame, Notre Dame, Indiana 46556, United States*

Alejandro J. Gonzalez − *Department of Biology, University of Notre Dame, Notre Dame, Indiana 46556, United States*

Tam T. Bui − *Centre for Biomolecular Spectroscopy and Randall Division of Cell and Molecular Biophysics, King's College London, London SE1 1UL, United Kingdom*

Victoria A. Ploplis − *Department of Chemistry and Biochemistry and W.M. Keck Center for Transgene Research, University of Notre Dame, Notre Dame, Indiana 46556, United States*

Francis J. Castellino − *Department of Chemistry and Biochemistry and W.M. Keck Center for Transgene Research, University of Notre Dame, Notre Dame, Indiana 46556, United States*

Albert Siryaporn − *Department of Physics and Astronomy and Department of Molecular Biology and Biochemistry, University of California Irvine, Irvine, California 92697, United States*

Mayland Chang − *Chemistry Biology Biochemistry Interface and Department of Chemistry and Biochemistry, University of Notre Dame, Notre Dame, Indiana 46556, United States;* orcid.org/0000-0002-4333-3775

J. Mark Sutton − *Technology Development Group, National Infection Service, Public Health England, Salisbury SP4 0JG, U.K.*

A. James Mason − *Institue of Pharmaceutical Science, School of Cancer & Pharmaceutical Science, King's College London, London SE1 9NH, United Kingdom;* orcid.org/0000-0003-0411-602X

Complete contact information is available at: https://pubs.acs.org/10.1021/acsptsci.0c00001

Author Contributions

F.R.F., G.M., J.M.S., C.K.H., A.S., M.C., A.J.M., V.A.P., F.J.C., and S.W.L. designed the overall project and experimental aims. F.R.F., G.M., M.C., J.J., I.P.F., P.D.S., R.D.B., H.M.V., J.N.R., V.R.K., A.J.G., and T.T.B. performed experimental work and analyzed results. F.R.F., A.J.M., and S.W.L. wrote the paper. All authors contributed to proofreading and editing the paper.

Funding

This work was supported by a National Institutes of Health (NIH) Innovator Grant (DP2OD008468−01) awarded to S.W.L. and NIH Grant R21AI139968 to A.S.

Notes

The authors declare no competing financial interest.

■ ACKNOWLEDGMENTS

FRF is supported by the NSF-GRFP, GEM Fellowship Award, and the CBBI Internship Travel Award. We would also like to thank Dr Katie Hopkins in the HCAI & AMR Division, National Infection Service, Public Health England, for providing some of the MDR Gram negative strains used in these studies. TEM work was performed at the University of California Irvine Materials Research Institute (IMRI) with technical support from Dr. Li Xing.

■ REFERENCES

(1) Cotter, P. D., Ross, R. P., and Hill, C. (2013) Bacteriocins - a Viable Alternative to Antibiotics? *Nat. Rev. Microbiol. 11* (2), 95−105.

(2) Fields, F. R., Lee, S. W., and McConnell, M. J. (2017) Using Bacterial Genomes and Essential Genes for the Development of New Antibiotics. *Biochem. Pharmacol. 134*, 74−86.

(3) Donia, M. S., Cimermancic, P., Schulze, C. J., Wieland Brown, L. C., Martin, J., Mitreva, M., Clardy, J., Linington, R. G., and Fischbach, M. A. (2014) A Systematic Analysis of Biosynthetic Gene Clusters in the Human Microbiome Reveals a Common Family of Antibiotics. *Cell 158* (6), 1402−1414.

(4) Murinda, S. E., Rashid, K. A., and Roberts, R. F. (2003) In Vitro Assessment of the Cytotoxicity of Nisin, Pediocin, and Selected Colicins on Simian Virus 40−Transfected Human Colon and Vero Monkey Kidney Cells with Trypan Blue Staining Viability Assays. *J. Food Prot. 66* (5), 847−853.

(5) van Staden, A. D., Brand, A. M., and Dicks, L. M. T. (2012) Nisin F-Loaded Brushite Bone Cement Prevented the Growth of Staphylococcus Aureus in Vivo. *J. Appl. Microbiol. 112* (4), 831−840.

(6) Sánchez-Hidalgo, M., Montalbán-López, M., Cebrián, R., Valdivia, E., Martínez-Bueno, M., and Maqueda, M. (2011) AS-48 Bacteriocin: Close to Perfection. *Cell. Mol. Life Sci. 68*, 2845−2857.
(7) Gómez, N. C., Abriouel, H., Grande, J., Pulido, R. P., and Gálvez, A. (2012) Effect of Enterocin AS-48 in Combination with Biocides on Planktonic and Sessile Listeria Monocytogenes. *Food Microbiol. 30*, 51−58.
(8) Galvez, A., Gimenez-Gallego, G., Maqueda, M., and Valdivia, E. (1989) Purification and Amino Acid Composition of Peptide Antibiotic AS-48 Produced by Streptococcus (Enterococcus) Faecalis Subsp. Liquefaciens S-48. *Antimicrob. Antimicrob. Agents Chemother. 33* (4), 437−441.
(9) Angeles Jiménez, M., Barrachi-Saccilotto, A. C., Valdivia, E., Maqueda, M., and Rico, M. (2005) Design, NMR Characterization and Activity of a 21-Residue Peptide Fragment of Bacteriocin AS-48 Containing Its Putative Membrane Interacting Region. *J. Pept. Sci. 11* (1), 29−36.
(10) Montalbán-López, M., Martínez-Bueno, M., Valdivia, E., and Maqueda, M. (2011) Expression of Linear Permutated Variants from Circular Enterocin AS-48. *Biochimie 93* (3), 549−555.
(11) Fields, F. R., Carothers, K. E., Balsara, R. D., Ploplis, V. A., Castellino, F. J., and Lee, S. W. (2018) Rational Design of Syn-Safencin, a Novel Linear Antimicrobial Peptide Derived from the Circular Bacteriocin Safencin AS-48. *J. Antibiot. 71*, 592.
(12) Fjell, C. D., Hiss, J. A., Hancock, R. E. W., and Schneider, G. (2012) Designing Antimicrobial Peptides: Form Follows Function. *Nat. Rev. Drug Discovery 11* (1), 37−51.
(13) Brogden, K. A. (2005) Antimicrobial Peptides: Pore Formers or Metabolic Inhibitors in Bacteria? *Nat. Rev. Microbiol. 3*, 238.
(14) Xhindoli, D., Pacor, S., Benincasa, M., Scocchi, M., Gennaro, R., and Tossi, A. (2016) The Human Cathelicidin LL-37 — A Pore-Forming Antibacterial Peptide and Host-Cell Modulator ☆. *Biochim. Biophys. Acta, Biomembr. 1858*, 546−566.
(15) Cruz, V. L., Ramos, J., Melo, M. N., and Martinez-Salazar, J. (2013) Bacteriocin AS-48 Binding to Model Membranes and Pore Formation as Revealed by Coarse-Grained Simulations. *Biochim. Biophys. Acta, Biomembr. 1828*, 2524−2531.
(16) Klocek, G., Schulthess, T., Shai, Y., and Seelig, J. (2009) Thermodynamics of Melittin Binding to Lipid Bilayers. Aggregation and Pore Formation. *Biochemistry 48* (12), 2586−2596.
(17) Manzo, G., Ferguson, P. M., Gustilo, V. B., Ali, H., Bui, T. T., Drake, A. F., Atkinson, A., Batoni, G., Lorenz, C. D., and Phoenix, D. A., et al. (2018) Minor Sequence Modifications in Temporin B Cause Drastic Changes in Antibacterial Potency and Selectivity by Fundamentally Altering Membrane Activity, *BioRxiv*,
(18) Manzo, G., Ferguson, P. M., Hind, C. K., Clifford, M., Gustilo, V. B., Ali, H., Bansal, S. S., Bui, T. T., Drake, A. F., Atkinson, R. A., Sutton, J. M., Lorenz, C. D., Phoenix, D. A., and Mason, A. J. (2019) ParTemporin L and aurein 2.5 have identical. *Sci. Rep. 9*, No. 10934.
(19) Ashrafuzzaman, M., Andersen, O. S., and McElhaney, R. N. (2008) The Antimicrobial Peptide Gramicidin S Permeabilizes Phospholipid Bilayer Membranes without Forming Discrete Ion Channels. *Biochim. Biophys. Acta, Biomembr. 1778* (12), 2814−2822.
(20) Liu, B., Chia, D., Csizmok, V., Farber, P., Forman-Kay, J. D., and Gradinaru, C. C. (2014) The Effect of Intrachain Electrostatic Repulsion on Conformational Disorder and Dynamics of the Sic1 Protein. *J. Phys. Chem. B 118* (15), 4088−4097.
(21) Tosatto, L., Andrighetti, A. O., Plotegher, N., Antonini, V., Tessari, I., Ricci, L., Bubacco, L., and Dalla Serra, M. (2012) Alpha-Synuclein Pore Forming Activity upon Membrane Association. *Biochim. Biophys. Acta, Biomembr. 1818* (11), 2876−2883.
(22) Strandberg, E., Zerweck, J., Horn, D., Pritz, G., Berditsch, M., Bürck, J., Wadhwani, P., and Ulrich, A. S. (2015) Influence of Hydrophobic Residues on the Activity of the Antimicrobial Peptide Magainin 2 and Its Synergy with PGLa. *J. Pept. Sci. 21* (5), 436−445.
(23) Cowles, K. N., Moser, T. S., Siryaporn, A., Nyakudarika, N., Dixon, W., Turner, J. J., and Gitai, Z. (2013) The Putative Poc Complex Controls Two Distinct Pseudomonas Aeruginosa Polar Motility Mechanisms. *Mol. Microbiol. 90* (5), 923−938.
(24) Cowles, K. N., and Gitai, Z. (2010) Surface Association and the MreB Cytoskeleton Regulate Pilus Production, Localization and Function in Pseudomonas Aeruginosa. *Mol. Microbiol. 76* (6), 1411−1426.
(25) Zerweck, J., Strandberg, E., Kukharenko, O., Reichert, J., Bürck, J., Wadhwani, P., and Ulrich, A. S. (2017) Molecular Mechanism of Synergy between the Antimicrobial Peptides PGLa and Magainin 2. *Sci. Rep. 7* (1), 1−21.
(26) Nissen-Meyer, J., Oppegård, C., Rogne, P., Haugen, H. S., and Kristiansen, P. E. (2010) Structure and Mode-of-Action of the Two-Peptide (Class-IIb) Bacteriocins. *Probiotics Antimicrob. Probiotics Antimicrob. Proteins 2* (1), 52−60.
(27) Kjos, M., Oppegard, C., Diep, D. B., Nes, I. F., Veening, J. W., Nissen-Meyer, J., and Kristensen, T. (2014) Sensitivity to the Two-Peptide Bacteriocin Lactococcin G Is Dependent on UppP, an Enzyme Involved in Cell-Wall Synthesis. *Mol. Microbiol. 92* (6), 1177−1187.

https://dx.doi.org/10.1021/acsptsci.0c00001
ACS Pharmacol. Transl. Sci. 2020, 3, 418−424